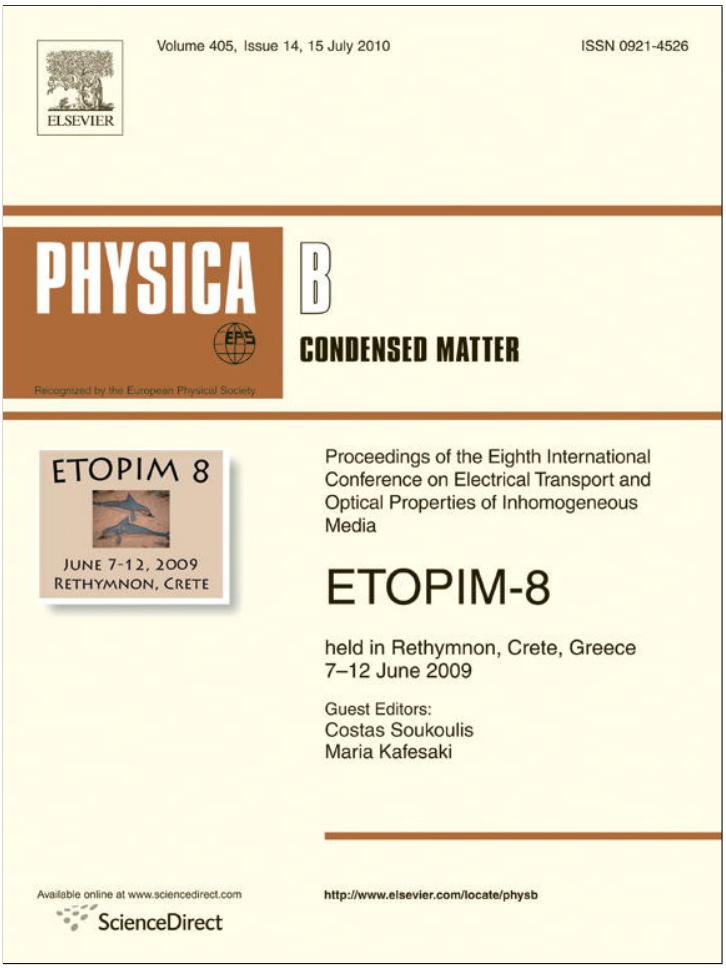

Physica B 405 (2010) 2967–2971

Contents lists available at ScienceDirect

Physica B

journal homepage: www.elsevier.com/locate/physb

# Plasmonic nanostructures and optical metamaterials: Studies by the layer-multiple-scattering method

N. Stefanou [a,*], N. Papanikolaou [b], C. Tserkezis [a]

[a] Section of Solid State Physics, University of Athens, Panepistimioupolis Zografou, GR-157 84 Athens, Greece
[b] Institute of Microelectronics, NCSR "Demokritos", GR-153 10 Athens, Greece

ARTICLE INFO

*Keywords:*
Plasmon
Metamaterial
Nanoantenna
Metallodielectric nanosandwich
Multiple scattering

ABSTRACT

We apply the layer-multiple-scattering method to study the optical properties of different plasmonic architectures; namely two- and three-dimensional periodic arrays of metallic nanocylinders and of metallodielectric nanosandwiches. These structures exhibit various types of collective plasmonic resonances, tunable over a broad spectral range from infrared to visible frequencies, which cause large enhancement of the local field and give rise to interesting phenomena that we discuss and provide a consistent interpretation of the underlying physics. We analyze extinction spectra of finite slabs of the structures under consideration and explain the different spectral features. In relation to optical metamaterials, we deduce effective electromagnetic parameters by the *S*-matrix retrieval procedure for single- and multi-layer slabs of periodic arrays of metallodielectric nanosandwiches and propose a method to resolve ambiguities in the determination of the effective refractive index, which become prominent for thick slabs, based on the complex band structure of the corresponding infinite crystal.


## 1. Introduction

In the last years, increasing amount of attention has been directed toward the assembly of metal nanoparticle building blocks into ordered structures for diverse applications that include, among others, (bio)sensing and optoelectronic devices [1–3]. The optical properties of such isolated particles are more or less well understood. However, this is clearly not the case with metal nanoparticle aggregates, because there are often complicating factors in analyzing relevant experiments and understanding the underlying physics, for example, the presence of a supporting substrate, a solvent layer, and strong electromagnetic (EM) coupling between the different building units. All of these factors motivate the need for accurate and computationally fast theoretical methods that can provide a full electrodynamic description of metallodielectric nanostructures of arbitrary shape and size, subject to a complex dielectric environment, thus allowing for the theoretical design and optimization of novel functional optical nanodevices.

Standard software packages based on the straightforward numerical solution of Maxwell equations using, e.g., finite-element or finite-difference time-domain techniques are valuable tools in the study of complex EM structures. The discrete dipole approximation method is also a widely used technique for assessing and evaluating the optical wave interaction with a (nano)structure. This method does not include an explicit multipole representation. Instead, it describes the optical properties of the building units in terms of dipole interactions of a huge dipole array that mimics the electrodynamic response of the actual particles. However, the above brute-force methods are rather time consuming and do not always allow to gain physical insight. Alternatively, an elegant computational methodology, the so-called extended layer-multiple-scattering method [4], offers unique advantages for investigating the optical properties of metallodielectric systems that contain periodic arrays of particles (scatterers) and homogeneous slabs. It is computationally fast, accurate, and allows for a direct physical interpretation of the results since the properties of the composite system are obtained from those of its building units and thus one can easily analyze the underlying physics. Moreover, contrary to traditional band-structure or time-domain techniques, the extended layer-multiple-scattering method proceeds at a given frequency, i.e., it is an "on-shell" method and, therefore, it is ideally suited for plasmonic structures containing strongly dispersive and absorptive elements made of metallic materials. Besides the complex band structure of a three-dimensional (3D) photonic crystal, associated with a given crystallographic plane, the method allows one to calculate, also, the transmission, reflection and absorption coefficients of an EM wave incident at a given angle on a finite slab of the crystal and, therefore, it can describe an actual transmission experiment. It is worth-noting that periodicity in the direction perpendicular to

* Corresponding author. Tel.: +30 210 7276762; fax: +30 210 7276711.
*E-mail addresses:* nstefan@phys.uoa.gr (N. Stefanou), N.Papanikolaou@imel.demokritos.gr (N. Papanikolaou), ctserk@phys.uoa.gr (C. Tserkezis).

0921-4526/$ - see front matter © 2010 Elsevier B.V. All rights reserved.
doi:10.1016/j.physb.2010.01.015

the layers is not required: the layers must only have the same two-dimensional (2D) periodicity.

In the present paper, we apply the extended layer-multiple-scattering method to study the optical response of different metallodielectric architectures, namely 2D and 3D periodic structures of cylindrical metallic nanoantennas and of metal–dielectric–metal nanodisks in a sandwich-like configuration. These systems exhibit various types of collective plasmonic resonances, tunable over a broad spectral range from infrared to visible frequencies, which cause large enhancement of the local field and give rise to a plethora of interesting phenomena, such as hybridization-induced frequency gaps, broad-band absorption, artificial optical magnetism, etc. Some of these effects are discussed here and a consistent interpretation of the underlying physical mechanisms is provided.

## 2. Method of calculation

Our calculations are based on the extended layer-multiple-scattering method, which was presented in detail elsewhere [4]. Here we restrict ourselves to a brief description of the main points of the method.

The structures that can be dealt with by this method may consist of successive, possibly different, layers of scatterers arranged with the same 2D periodicity. The properties of the individual scatterers enter only through the corresponding $T$ matrix which, for homogeneous spherical particles, is given by the closed-form solutions of the Mie-scattering problem, while for scatterers of arbitrary shape it is calculated numerically by the extended-boundary-condition method [5]. At a first step, in-plane multiple scattering is evaluated in a spherical-wave basis using proper propagator functions. Subsequently, interlayer scattering is calculated in a plane-wave basis through appropriate reflection and transmission matrices. The scattering $S$ matrix of a multilayer slab, which transforms the incident into the outgoing wave field, is obtained by combining the reflection and transmission matrices of the component layers. The ratio of the transmitted or reflected energy flux to the energy flux associated with the incident wave defines the transmittance or reflectance of the slab, respectively.

On the other hand, for a 3D crystal consisting of an infinite periodic sequence of layers, stacked along the $z$ direction, applying the Bloch condition for the wave field in the region between two consecutive unit slabs leads to an eigenvalue equation, which gives the $z$ component of the Bloch wave vector, $k_z$, for given frequency $\omega$ and in-plane reduced wave vector component $\mathbf{k}_\parallel$, which are conserved quantities in the scattering process. The eigenvalues $k_z(\omega,\mathbf{k}_\parallel)$, looked upon as functions of real $\omega$, define, for each $\mathbf{k}_\parallel$, lines (sometimes they are called real-frequency lines) in the complex $k_z$ plane. Taken together they constitute the complex band structure of the infinite crystal associated with the given crystallographic plane. A line of given $\mathbf{k}_\parallel$ may be real (in the sense that $k_z$ is real) over certain frequency regions, and be complex (in the sense that $k_z$ is complex) for $\omega$ outside these regions. It turns out that for given $\mathbf{k}_\parallel$ and $\omega$, out of the eigenvalues $k_z(\omega,\mathbf{k}_\parallel)$ none or, at best, a few are real and the corresponding eigenvectors represent propagating modes of the EM field in the given infinite crystal. The remaining eigenvalues $k_z(\omega,\mathbf{k}_\parallel)$ are complex and the corresponding eigenvectors represent evanescent waves. These have an amplitude which increases exponentially in the positive or negative $z$ direction and, unlike the propagating waves, do not exist as physical entities in the infinite crystal. However, they are an essential part of the physical solutions of the EM field in a slab of finite thickness. A region of frequency where propagating waves do not exist, for given $\mathbf{k}_\parallel$, constitutes a frequency gap of the EM field for the given $\mathbf{k}_\parallel$. If over a frequency region no propagating wave exists whatever the value of $\mathbf{k}_\parallel$, then this region constitutes an absolute frequency gap.

In order to ensure adequate convergence in our calculations for the structures under consideration, we truncate the spherical-wave expansions at $\ell_{\max}=12$ and take into account 151 2D reciprocal lattice vectors in the relevant plane-wave expansions, while the single-particle scattering $T$ matrix is evaluated with $\ell_{\mathrm{cut}}=16$ and a Gaussian quadrature integration formula with 6000 points.

## 3. Nanoantenna arrays

Optical antennas, operating through the excitation of plasmon modes localized at properly designed metallic nanoparticles [6], are fundamental devices for directing an incoming light wave to subwavelength dimensions. Moreover, optical antennas characterized by strong plasmon resonances provide an important mechanism for locally amplifying the EM field. This characteristic is of particular interest to enhance a weak optical response, e.g., in single molecule fluorescence and Raman scattering, or trigger nonlinear effects. In the simple case of noble-metal nanospheres, the extinction spectrum is dominated by strong dipole plasmon resonances at visible wavelengths. For elongated particles, the threefold degeneracy of these modes is lifted and one obtains a predominant nondegenerate longitudinal mode at longer wavelengths as well as doubly degenerate transverse and other modes of mixed character at shorter wavelengths. The longitudinal resonance can be easily tuned by properly choosing the particle aspect ratio [7]. Therefore, elongated metallic nanoparticles, such as spheroids or cylinders, can be used as efficient and tunable optical antennas for manipulating light at the nanoscale and tailoring the light-matter interaction. In this section, we report on the optical response of planar periodic arrays of free standing aligned silver nanocylinders, by means of full electrodynamic calculations using the extended layer-multiple-scattering method [4]. For the permittivity of silver we interpolate to the bulk values measured by Johnson and Christy [8].

The fundamental longitudinal resonance wavelength of an isolated silver nanocylinder increases almost linearly with the particle aspect ratio. Interestingly, this resonance appears at wavelengths much longer than those of an ideal half-wave dipole antenna ($L=\lambda/2$). This is explained as follows. At optical frequencies the simple wavelength scaling $L=\lambda/2$ breaks down because incident radiation is no longer perfectly reflected from the metal's surface. Instead, the wave field penetrates into the metal and gives rise to surface-plasma oscillations. Hence, at optical frequencies an antenna does not respond to the external wavelength, $\lambda$, but to an effective wavelength, $\lambda_{\mathrm{eff}}$, which depends on the material properties [9].

We consider square arrays of silver nanocylinders, of diameter $d=20\,\mathrm{nm}$ and length $L=50\,\mathrm{nm}$, with different lattice constants, $a_0$, in air. Interaction between plasmons of the individual particles gives rise to corresponding collective plasmon modes, which manifest themselves as peaks in the extinction spectra (extinction = negative logarithm of the transmittance) of these arrays. Expectedly, under illumination at normal incidence or at an angle with s-polarized light, the longitudinal modes are not excited since, in these cases, the electric field of the incident EM wave oscillates perpendicularly to the particle axis. At oblique incidence, a p-polarized incident wave excites both longitudinal and transverse collective plasmon modes, as can be seen in Fig. 1. By increasing the angle of incidence, the component of the electric field of the p-polarized incident wave along the cylinders becomes larger, and thus the longitudinal plasmon modes are excited more efficiently leading to stronger resonance

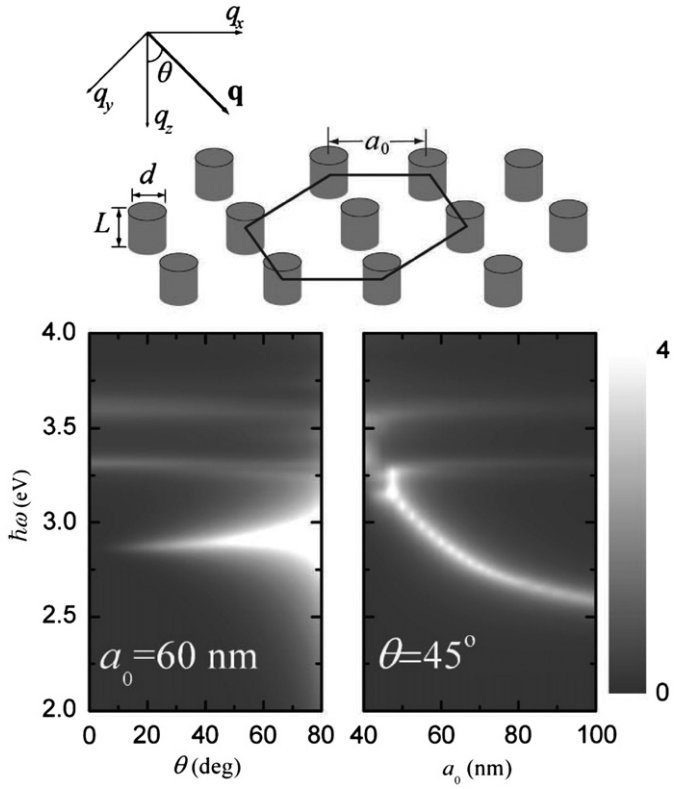


**Fig. 1.** Extinction spectra of hexagonal arrays, with lattice constant $a_0$, of free standing, aligned silver nanocylinders ($d=20\,\text{nm}, L=50\,\text{nm}$), under illumination with a p-polarized plane wave incident at an angle $\theta$ with respect to the cylinder axis.

peaks in the extinction spectrum. It is worth-noting that the peak positions do not vary much with the angle of incidence, thus implying a relatively weak dispersion of the corresponding collective plasmon modes. However, as the lattice constant decreases and the nanocylinders approach each other, their interaction is enhanced and leads to large shifts of the low-frequency collective longitudinal plasmon modes. For $a_0 = 100\,\text{nm}$, the extinction peaks about 2.59 and 3.32 eV, 3.61 eV essentially correspond to the longitudinal and transverse plasmon modes, respectively, of the isolated nanocylinder. As the lattice constant decreases, interparticle coupling leads to a strong blue shift of the low-frequency longitudinal resonance while the position of the high-frequency resonances remains almost unchanged. Similar results are obtained for cylinders with larger aspect ratios, where the tunability of the longitudinal resonance is further extended to the region of infrared frequencies.

Our results are in line with recent experimental and theoretical studies on arrays of longer gold nanorods, fabricated by electrodeposition into thin nanoporous anodized aluminum oxide templates [10,11]. It becomes clear from the above that ordered arrays of metallic nanocylinders provide the opportunity for engineering collective plasmon modes that can be easily tuned throughout the spectrum of visible and infrared frequencies by a proper choice of the geometric parameters of the structure.

## 4. Structures of metal–dielectric–metal nanosandwiches

Periodic assemblies of in-tandem pairs of metallic nanodisks separated by a dielectric spacer, so-called metal–dielectric–metal nanosandwiches, constitute a novel class of photonic metamaterials with intriguing optical properties. For example, such composite nanoparticles, also termed nanoburgers, provide impressive opportunities for engineering efficient surface-enhanced Raman scattering active substrates [12]. When two metallic nanodisks are brought into strong coupling in a sandwich-like configuration, plasmon hybridization results into a symmetric resonant mode, with the dipole moments of the nanodisks oscillating in phase, and an antisymmetric resonant mode, with the dipole moments oscillating with opposite phase. While the symmetric resonance has an electric dipolar character, the antisymmetric one is associated with a loop-like current in the nanodisk pair and thus a dipole magnetic moment [13]. 2D and 3D structures of such photonic metamolecules may exhibit a negative effective permeability in the region of the antisymmetric resonance, at visible and near-infrared frequencies [14], which is an essential ingredient in the design of negative-index metamaterials. Compared to pairs of rods or of cut-wires, the optical behavior of disk pairs is more isotropic because the latter are invariant under rotation about their axis. It is worth-noting that, contrary to the formation of bonding and antibonding electron orbitals in diatomic molecules, in a metal–dielectric–metal nanosandwich, the low-frequency hybrid plasmonic mode is antisymmetric and the high-frequency one is symmetric. This apparently counter-intuitive situation can be understood as follows. Charge oscillations associated with an electric-dipole plasmon mode in a single metallic nanodisk are sustained by restoring forces acting on the collectively displaced conduction-band electrons. In an in-tandem pair of such nanodisks, charge distribution leads to reduction of the appearing restoring forces in the configuration of the antisymmetric mode and enhancement in the case of the symmetric mode. Consequently, the eigenfrequency of the antisymmetric mode is lowered and that of the symmetric mode is raised, as shown schematically in Fig. 2. The situation is reversed if the two nanodisks are on the same plane.

Hybridization between the particle-plasmon modes of the two metallic nanodisks of a single nanosandwich can be studied by keeping their thickness fixed ($h_1 = h_3$) and varying the thickness $h_2$ of the dielectric spacer, in a relatively sparse array of nanosandwiches. Systematic calculations for 2D arrays of silver–silica–silver nanosandwiches show that (see Fig. 2), for very thin dielectric spacers, the extinction spectrum tends to a single-peak structure, which is essentially the particle-plasmon resonance in the corresponding array of homogeneous silver disks of double thickness. When the separation between silver disks in the nanosandwich is larger, the spectra exhibit two distinct peaks

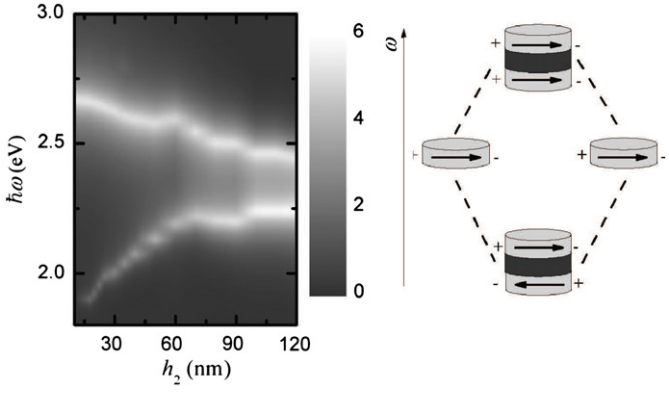


**Fig. 2.** Extinction spectra at normal incidence of hexagonal arrays, with lattice constant $a_0 = 200\,\text{nm}$, of silver–silica–silver nanosandwiches ($d = 100\,\text{nm}, h_1 = h_3 = 20\,\text{nm}$), for different values of spacer thickness, $h_2$, on a quartz substrate. For the permittivity of silver we interpolate to the bulk values measured by Johnson and Christy [8], while the permittivity of silica and quartz is taken equal to 2.13. Plasmon hybridization in a metal–dielectric–metal nanosandwich is schematically shown in the margin.

that originate from the excitation of the composite plasmon modes of the individual nanosandwiches, weakly interacting between them. With increasing thickness of the dielectric spacer, the high-frequency peak shifts to the red while the low-frequency peak shifts to the blue and gradually becomes more pronounced. It is worth-noting that the shift of the low-frequency antisymmetric mode is larger than that of the high-frequency symmetric mode. Our results are in good agreement with existing experimental data on isolated gold–silica–gold nanosandwiches [13]. The interaction between nanosandwiches increases as we reduce the lattice constant and is manifested as a small shift of the resonance peaks and more pronounced extinction [14].

We now consider multilayer structures of free standing metal–dielectric–metal nanosandwiches. In each layer, the nanosandwiches are arranged on a hexagonal lattice determined by the primitive vectors $\mathbf{a}_1 = a_0(1,0,0)$ and $\mathbf{a}_2 = a_0(1/2, \sqrt{3}/2, 0)$. We assume that the permittivity of the metallic material is described by the Drude permittivity, $\varepsilon_m = 1\text{-}\omega_p^2/\omega(\omega + i\gamma)$, where $\omega_p$ is the bulk plasma frequency and $\gamma$ a damping factor that accounts for dissipative losses. The nanosandwiches consist of two metallic nanodisks, of diameter $d = 5c/\omega_p$ and thickness $h_1 = h_3 = c/\omega_p$, separated by a silica spacer ($\varepsilon_{silica} = 2.13$) of thickness $h_2 = 2c/\omega_p$. Therefore, $h = h_1 + h_2 + h_3 = 4c/\omega_p$ is the total thickness of the nanosandwich. The stacking sequence is defined by $\mathbf{a}_3 = (a_0/2, a_0\sqrt{3}/2, h)$. We take $a_0 = 10c/\omega_p$.

The effective EM parameters of the multilayers under consideration, i.e., the permittivity and permeability functions of an equivalent homogeneous medium, are determined from the scattered field in the far zone, under plane wave illumination. At normal incidence, inverting the standard Fresnel equations, we obtain closed-form solutions for the effective refractive index, $n_{eff}$, and impedance, $z_{eff}$, in terms of the complex transmission and reflection coefficients, This so-called *S*-matrix retrieval procedure was first applied for metamaterial layers by O'Brien and Pendry [15] and Smith et al. [16], and later used by many research groups. It is worth-noting that the effective refractive index often remains ambiguous because of the multiple branches of the tangent function appearing in the expression of $n_{eff}$. For a slab of small thickness, e.g. one monolayer, it is usually the fundamental branch which is relevant. However, for thicker slabs, higher branches may lie arbitrarily close to each other, making the selection of the correct branch difficult, as pointed out by others as well [16,17], while possible discontinuities due to resonances complicate the determination of an effective refractive index. Here we use the refractive index deduced from the complex photonic band structure of the corresponding infinite crystal, $c[\mathrm{Re}\, k_z + i\, \mathrm{Im}\, k_z]/\omega$ ($c$ is the velocity of light in vacuum), as a reference for choosing the proper branch, especially in the case of relatively thick slabs.

The effective permittivity and permeability of the slab are subsequently obtained through the relations $\varepsilon_{eff} = n_{eff}/z_{eff}$ and $\mu_{eff} = n_{eff} z_{eff}$. Obviously, $\varepsilon_{eff}$ and $\mu_{eff}$ do not describe the wave field inside the actual crystal where, at a given frequency, it has the form of a Bloch wave rather than a simple plane wave. However, the effective parameters must be such that these two waves obey the same dispersion relation and, therefore, have the same group (and phase) velocity. This remark is of course meaningful only if there is a single dominant relevant Bloch mode at the given frequency. Moreover, in order for an effective-medium description to be applicable, the wavelength in the embedding medium must be much larger than the in-plane period of the lattice. This condition ensures that there is only a single propagating mode of the scattered EM field by a finite slab of the structure, corresponding to outgoing waves (refracted and reflected beams). All other components of the wave field (diffracted beams) are evanescent.

In Fig. 3 we display the retrieved $\mu_{eff}$, for slabs one-, two- and eight-layers thick, which clearly converges with increasing slab thickness and exhibits a resonant behavior about the frequency of the antisymmetric plasmon modes. It can be seen that, even assuming that the building units of the structure are non-absorptive with purely real permittivities and permeabilities, the *S*-matrix retrieval method leads to a non-zero imaginary part for $\mu_{eff}$ (and also for $\varepsilon_{eff}$ that we do not show here) in the frequency region of the resonance, with $\mathrm{Im}\, \varepsilon_{eff} < 0$ and $\mathrm{Im}\, \mu_{eff} > 0$. However, the retrieval procedure itself ensures that the values of $\varepsilon_{eff}$ and $\mu_{eff}$ are such that the absorption of each effective slab vanishes at any frequency. In some sense, it is not possible that the effective slab complies with the strong restriction to reproduce exactly the transmission and reflection coefficients of the actual metamaterial slab, with real functions $\varepsilon_{eff}(\omega)$ and $\mu_{eff}(\omega)$ in the resonance region. To make this possible, one has to assume complex functions with negative $\mathrm{Im}\, \varepsilon_{eff}$ and positive $\mathrm{Im}\, \mu_{eff}$, i.e., some fictitious dielectric gain, which counterbalances the fictitious magnetic losses. Obviously, this occurs for given slab thickness, specific characteristics of the incident field, etc. and, therefore, $\varepsilon_{eff}$ and $\mu_{eff}$ have not the meaning of inherent material parameters [18]. If absorptive losses in the metallic material are taken into account, the resonance structures become smoother and more extended in frequency while the region of negative permeability shrinks and almost disappears, as shown in the right-hand panel of Fig. 3.

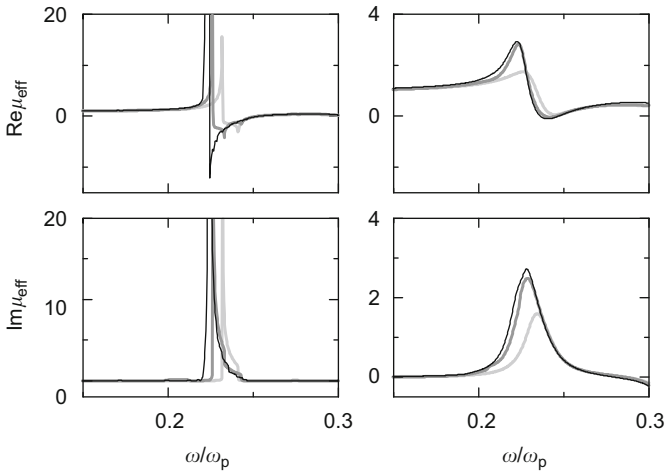


**Fig. 3.** Effective permeability of one- (light gray lines), two- (gray lines) and eight- (black lines) layers thick slabs of the structure under consideration, at normal incidence. Left: without losses ($\gamma = 0$). Right: with losses ($\gamma = 0.025\, c/\omega_p$).

## 5. Conclusion

In summary, we reported on the optical response of plasmonic structures, namely 2D and 3D ordered arrays of metallic nanocylinders and of metal–dielectric–metal nanosandwiches, by means of full electrodynamic calculations using the extended layer-multiple-scattering method and showed that the method retains its high efficiency and accuracy even in cases of particles with edges and strong deviation from the spherical shape. More specifically, we investigated hexagonal arrays of silver nanoantennas of cylindrical shape and demonstrated the existence of collective plasmonic modes of different character. In particular, we showed that such longitudinal modes exhibit polarization selectivity and tunability throughout the range of visible and infrared frequencies, properties which are very useful for filtering and sensing applications. Moreover, we reported on single- and multi-layer architectures of ordered assemblies of silver–silica–silver nanosandwiches. We showed that plasmon hybridization leads to a double-peak structure in the extinction spectrum of such a monolayer on a quartz substrate, with

a symmetric and an antisymmetric resonance that can be tailored by properly changing the geometric parameters involved. Our results corroborate that these structures can also be useful for practical applications, e.g. as chemical and biological sensors, while the presence of an antisymmetric resonance makes metallodielectric nanosandwiches potential candidates as building units in the design of novel negative-index metamaterials. In this respect, we analyzed a specific design of layered periodic structure of metal–dielectric–metal nanosandwiches, which exhibits strong artificial optical magnetism, and examined the variation of its resonant magnetic response as successive layers are stacked together to build a 3D crystal. We deduced effective EM parameters by the *S*-matrix retrieval procedure and introduced a method to resolve ambiguities in the determination of the effective refractive index, which become prominent for thick slabs, based on the complex band structure of the corresponding infinite crystal.

## Acknowledgment

This work was supported by the research programme "Kapodistrias" of the University of Athens.

## References

[1] W.L. Barnes, A. Dereux, T.W. Ebbesen, Nature (London) 424 (2003) 824.
[2] E. Ozbay, Science 311 (2006) 189.
[3] E. Fort, S. Grésillon, J. Phys. D Appl. Phys. 41 (2008) 013001.
[4] G. Gantzounis, N. Stefanou, Phys. Rev. B 73 (2006) 035115.
[5] M.I. Mishchenko, L.D. Travis, A.A. Lacis, Scattering, Absorption, and Emission of Light by Small Particles, Cambridge University Press, Cambridge, 2002.
[6] P. Mühlschlegel, H.J. Eisler, O.J.F. Martin, B. Hecht, D.W. Pohl, Science 308 (2005) 1607.
[7] S. Eustis, M.A. El-Sayed, Chem. Soc. Rev. 35 (2006) 209.
[8] P.B. Johnson, R.W. Christy, Phys. Rev. B 6 (1972) 4370.
[9] L. Novotny, Phys. Rev. Lett. 98 (2007) 266802.
[10] G.A. Wurtz, W. Dickson, D. O'Connor, R. Atkinson, W. Hendren, P. Evans, R. Pollard, A.V. Zayats, Opt. Exp. 16 (2008) 7460.
[11] R. Kullock, W. Hendren, A. Hille, S. Grafstrôm, P. Evans, R. Pollard, R. Atkinson, L. Eng, Opt. Exp. 16 (2008) 21671.
[12] K.H. Su, S. Durant, J.M. Steele, Y. Xiong, C. Sun, X. Zhang, J. Phys. Chem. B 110 (2006) 3964.
[13] A. Dmitriev, T. Pakizeh, M. Käll, D.S. Sutherland, Small 3 (2007) 294.
[14] C. Tserkezis, N. Papanikolaou, G. Gantzounis, N. Stefanou, Phys. Rev. B 78 (2008) 165114.
[15] S. O'Brien, J.B. Pendry, J. Phys. Condens. Matter 1 (2002) 4035.
[16] D.R. Smith, S. Schultz, P. Markoš, C.M. Soukoulis, Phys. Rev. B 65 (2002) 195104.
[17] X. Chen, T.M. Grzegorczyk, B.I. Wu, J. Pacheco Jr., J.A. Kong, Phys. Rev. E 70 (2004) 016608.
[18] A.L. Efros, Phys. Rev. E 70 (2004) 048602.